Shape from Focus System

Shree K. Nayar

Department of Computer Science, Columbia University, New York, N.Y. 10027

Abstract

The shape-from-focus method described in this paper uses different focus levels to obtain a sequence of object images. The sum-modified-Laplacian (SML) operator is developed to provide local measures of the quality of image focus. The operator is applied to the image sequence of the object to determine a set of focus measures at each image point. A model is developed to describe the variation of focus measure values due to defocusing. This model is used by a depth estimation algorithm to interpolate focus measure values and obtain accurate depth estimates. We conclude with a description of a fully automated system that has been implemented using an optical microscope and tested on a variety of industrial samples.

1 Introduction

All surfaces encountered in practice are rough at some level detail. At that level, they exhibit high-frequency spatial surface variations that are often random in nature. In many vision applications, the spatial surface variations are comparable in dimensions to the resolution of the imaging system. Image intensities produced by such surfaces vary in an unpredictable manner from one sensor element (pixel) to the next. Hence, it is difficult to obtain dense and accurate surface shape information by using existing passive or active sensing techniques such as stereo, shape from shading, and structured light. Therefore, a practical and reliable solution to this rather difficult extraction problem is desirable. In this paper, we develop a shape extraction technique that uses focus analysis to recover dense depth maps of surfaces with complex reflectance and roughness properties.

1.1 Background

Previously, focus analysis has been used to automatically focus imaging systems or to obtain *sparse* depth information from the observed scene. Horn [1] proposed focusing imaging systems by using the Fourier transform and analyzing the frequency spectrum of the image. Tenenbaum [2] developed the gradient magnitude maximization method that uses the sharpness of edges to optimize focus quality. A modification to this approach was later proposed by Jarvis [3]. Jarvis formulated the sum-modulus-difference as the sum of the first intensity differences between neighboring pixels along a scan-line and used it as a measure of focus quality. Several auto-focusing algorithms were implemented and tested by Schlag et.al. [4].

More recently, Krotkov [5] evaluated and compared the performance of different focus criterion functions. Krotkov also proposed a method to estimate the depth of an image area. Pentland [6] suggested estimating the depth of image points by evaluating image blur due to defocusing. A similar approach was applied to edge points by Grossmann [7]. Darrell and Wohn [8] have developed a depth from focus method that obtains an image sequence of a scene by varying the focus level, and uses Laplacian and Gaussian pyramids to calculate depth. Subbarao [9] suggests the change of intrinsic camera parameters to recover the depth map of a scene.

1.2 Shape from Focus

In this paper, we develop a shape-from-focus method. In contrast to previous work in this area, we avoid the following approaches.

- We do not attempt to estimate depth from a pair of images by evaluating local estimates of the blurring function. The accuracy of such a method is greatly dependent on the blurring model used. The models used thus far are only approximations to the actual physical-optics model and therefore do not ensure high quality results.
- We do not apply our method to general scenes. Depth estimation based on focus analysis relies on the presence of high frequency brightness variation in the scene. General scenes often have areas with little or no brightness variation. For this reason, experiments in the past have only produced sparse depth information.

Here, we restrict ourselves to visibly rough surfaces that produce images with high frequency intensity variations. We review the image formation process and show that a defocused imaging system plays the role of a low-pass filter. The shape-from-focus method moves the unknown object with respect to the imaging system and obtains a sequence of images that correspond to different levels of object focus. The sum-modified-Laplacian (SML) operator is developed to measure the relative degree of focus between images. The operator is applied to the image sequence to obtain a set of focus measures at each image point. A model is developed that describes focus measure variations due to defocusing. This model is used to interpolate between a few focus measures to obtain accurate depth estimates.

0-8186-2855-3/92 $3.00 ©1992 IEEE

We have implemented a fully automated shape-from-focus system for inspecting microscopic objects that are upto a hundered microns in size. A motorized optical microscope is used to obtain a sequence of object images. Two results are produced by the recovery algorithm. The first is a focused image of the object that is reconstructed from the sequence of partially focused images. The second is a depth map of the object surface. The automated system has been applied to a variety of industrial samples. The results indicate that the method is capable of extracting dense and accurate shape information from a small number of object images.

2 Visibly Rough Surfaces

In the study of reflection, a rough surface is defined as one whose smallest spatial variations have dimensions that are much larger than the wavelength of the incident electromagnetic waves. This is the concept of optical roughness. In this paper, we introduce the notion of *visible roughness*; a surface is visibly rough if the dimensions of its spatial variations are comparable to the viewing area of individual elements (e.g. pixels) of the sensor (e.g. camera) used to observe the surface. The surface shown in Fig.1 is comprised of a large number of facets While the surface appears to have a smoothly varying global shape, $z(x, y)$, the orientation α of individual facets may deviate considerably from the mean surface orientation in the facet vicinity. Although facet orientations are dependent on the global shape of the surface and on the orientations of neighboring facets, they often exhibit some degree of randomness.

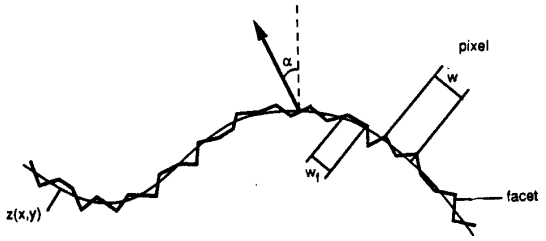

Figure 1: Surface roughness and sensor resolution.

Now, consider the image of a rough surface obtained using a finite resolution sensor. If the pixel width w is comparable to the facet width w_f, only one or few facets are viewed by each pixel. As a result of the randomness in facet orientations, image intensity values vary drastically and unpredictably from one pixel to the next. This is true for facets that are specular or diffuse in reflectance; the facet radiance in both cases is dependent on the angle of incident light. The surface therefore produces images that are rich in texture[1] and we say that the surface is *visibly rough*.

[1]The textures produced by visibly rough surfaces may be periodic, nearly periodic, or random. No assumptions are made regarding the type of texture.

3 Focused and Defocused Images

In this section, we briefly review the image formation process and describe defocused images as processed versions of focused images. Fig.2 shows the basic image formation geometry. All light rays that are radiated by the object point P and intercepted by the lens are refracted by the lens to converge at the point Q on the image plane. The relationship between the object distance o, focal distance of the lens f, and the image distance i, is given by the Gaussian lens law:

$$\frac{1}{o} + \frac{1}{i} = \frac{1}{f}. \tag{1}$$

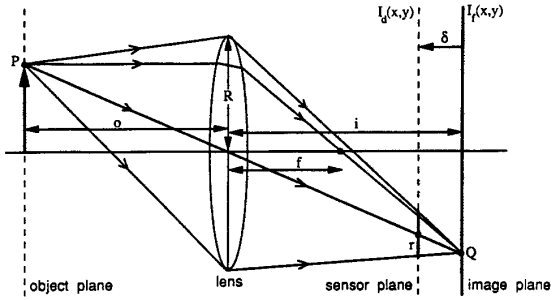

Figure 2: Formation of focused and defocused images.

Each point on the object plane is projected onto a single point on the image plane, thus causing a clear or *focused* image $I_f(x,y)$ to be formed on the image plane. If, however, the sensor plane does not coincide with the image plane and is displaced from it by a distance δ, the energy received from the object by the lens is distributed over a circular[2] patch on the sensor plane. Fig.2 may be used to establish the relationship between the radius r of the circular patch and the sensor displacement δ. From Fig.2 we find that:

$$r = \frac{\delta R}{i} \tag{2}$$

where R is the radius of the lens. It is also possible to convince oneself that the radius r of the circular patch is independent of P's location on the object plane. The distribution of light energy over the circular patch, or the *blurring function*, can be modeled using physical optics [6]. Very often, a two-dimensional Gaussian function is used to approximate the physical model [6] [9]. Then, the blurred or *defocused* image $I_d(x,y)$ formed on the sensor plane can be described as the result of convolving the focused image $I_f(x,y)$ with the blurring function $h(x,y)$:

$$I_d(x,y) = h(x,y) * I_f(x,y) \tag{3}$$

where:

$$h(x,y) = \frac{1}{2\pi\sigma_h^2} e^{-\frac{x^2+y^2}{2\sigma_h^2}} \tag{4}$$

[2]The shape of the patch also depends on the shape of the aperture of the imaging system. We are assuming the aperture to be circular.

where σ_h, the *spread parameter*, is assumed to be proportional to the radius r [6]. The constant of proportionality is dependent on the optics, sampling, etc. We will see shortly that the value of this constant is not important in our approach. Note that defocusing is observed for both positive and negative sensor displacements.

Now let us analyze the defocusing process in the frequency domain (u, v). If $I_F(u, v)$, $H(u, v)$, and $I_D(u, v)$ are the Fourier transforms of $I_f(x, y)$, $h(x, y)$, and $I_d(x, y)$, respectively, we can express eq. 3 as:

$$I_D(u, v) = H(u, v) . I_F(u, v) \tag{5}$$

where:

$$H(u, v) = e^{-\frac{u^2+v^2}{2}\sigma_h{}^2} \tag{6}$$

We see that $H(u, v)$ allows low frequencies to pass while it attenuates the high frequencies in the focused image. Furthermore, as the sensor displacement δ increases, the defocusing radius r increases, and the spread parameter σ_h increases. Hence defocusing is a *low-pass* filtering process where the bandwidth decreases with increase in defocusing.

From Fig.2, it is seen that a defocused image of the object can be obtained in three ways: by displacing the sensor with respect to the image plane, by moving the lens, or by moving the object with respect to the object plane. Moving the lens or sensor plane with respect to one another causes the following problems: (a) The magnification of the system varies, causing the image coordinates of focused points on the object to change, and (b) the area on the sensor plane over which light energy is distributed varies, causing a variation in image brightness. These effects are described in detail by Willson and Shafer [12]. In order to overcome these problems, we propose to vary the degree of focus by moving the object[3] with respect to a fixed configuration of the optical system and sensor. This approach ensures that, as the object moves, the magnification of imaging system is constant for the image areas that are perfectly focused. We further assume that the magnification remains constant for image areas that are marginally defocused. A more detailed analysis of this assumption is provided in [10]. This assumption will be used later while developing the depth estimation algorithm.

4 Shape from Focus: An Overview

Fig.3 shows an object of unknown shape placed on a translational stage. The reference plane shown corresponds to the initial position of the stage. The configuration of the optics and sensor defines a single plane, the "focused plane[4]," that is perfectly focused onto the sensor plane. The distance d_f between the focused and reference planes, and the displacement d of the stage with respect to the reference plane, are always known by measurement. Consider the surface element, s, that lies on the object surface, S. If the stage is moved towards the focused plane, the image of s will gradually increase in its degree of focus (high frequency content) and will be perfectly focused when s lies on the focused plane. Further movement of the element s will again increase the defocusing of its image. If we observe the image area corresponding to s and record the stage displacement $d = \overline{d}$ at the instant of maximum focus, we can compute the height d_s of s with respect to the stage as $d_s = d_f - \overline{d}$. In fact, we can use $\overline{d}$ to determine the distance of s from the focused plane, sensor plane, or any other coordinate system defined with respect to the imaging system. This procedure may be applied independently to all surface elements to obtain the shape of the entire surface S.

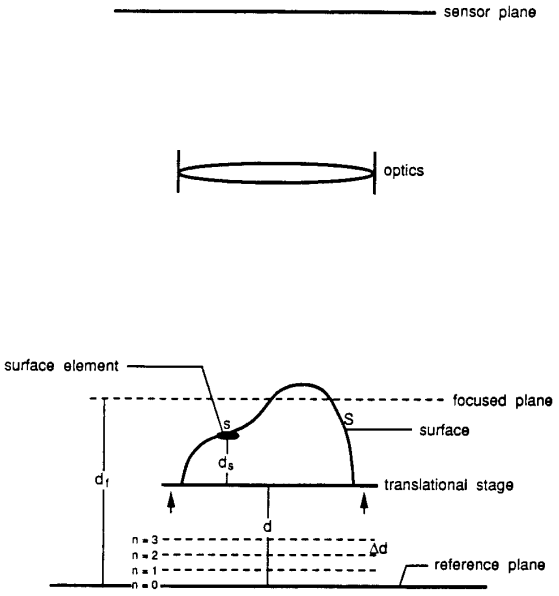

Figure 3: Shape from focus.

To automatically detect the instant of "best" focus, we will develop an image focus measure. In the above discussion, the stage motion and image acquisition were assumed to be continuous processes. In practice, however, it is not feasible to acquire and process such a large number of images in a reasonable amount of time. Therefore, we obtain only a finite number of images; the stage is moved in increments of Δd, and an image is obtained at each stage position ($d = n.\Delta d$). By studying the behavior of the focus measure, we develop an interpolation method that uses a small number of focus measures to compute accurate depth estimates.

5 A Focus Measure Operator

A few focus measure operators have been proposed and used in the past [5]. Generally, the objective has been to find an operator that behaves in a stable and robust manner over a variety of images such as images of indoor and outdoor scenes. Such an approach is essential while developing au-

[3] Object movement is easily realized in industrial and medical applications.

[4] The focused plane is the same as the object plane defined in the previous section. A different term is introduced here as the object does not necessarily lie on the focused plane.

tomatically focusing imaging systems that have to deal with general scenes. Bearing in mind that we are dealing with textured images, we develop an operator that is particularly well-suited to such images.

An interesting observation can be made regarding the application of focus measure operators. Eq. 3 relates a defocused image to a focused image using the blurring function. Assume that a focus measure operator $o(x,y)$ is applied (by convolution) to the defocused image $I_d(x,y)$. The result is a new image $r(x,y)$ that may be expressed as:

$$r(x,y) = o(x,y) * (h(x,y) * I_f(x,y)) \quad (7)$$

Since convolution is a linear operation, we can rewrite the above expression as:

$$r(x,y) = h(x,y) * (o(x,y) * I_f(x,y)) \quad (8)$$

Therefore, applying a focus measure operator to a defocused image is equivalent to defocusing a new image obtained by convolving the focused image with the focus measure operator. The focus measure operator only selects the frequencies in the focused image that will be attenuated due to defocusing. Since defocusing is a low-pass filtering process, its effects on the image are more pronounced and detectable if the image has strong high frequency content. An effective focus measure operator, therefore, must high-pass filter the image.

One way to high-pass filter an image is to determine its second derivative. For two-dimensional images, the *Laplacian* may be used:

$$\nabla^2 I = \frac{\partial^2 I}{\partial x^2} + \frac{\partial^2 I}{\partial y^2} \quad (9)$$

where $I(x,y)$ is the image intensity at the point (x,y). In frequency domain, applying the Laplacian $L(u,v)$ to the defocused image $I_D(u,v)$ (eq. 5) gives:

$$L(u,v).H(u,v).I_F(u,v) \quad (10)$$

where:

$$L(u,v).H(u,v) = -(u^2 + v^2).e^{-\frac{u^2+v^2}{2}\sigma_h^2} \quad (11)$$

For any given frequency (u,v), $|\ L.H\ |$ varies as a Gaussian function of the defocusing parameter σ_h. In general, however, the result would depend on the frequency distribution of the imaged scene. Though our texture is random, it may be assumed to have a set of dominant frequencies. Then, loosely speaking, each frequency is attenuated by a Gaussian function in σ_h and its width is determined by the frequency. Therefore, the result of applying the Laplacian operator may be expressed as a sum of Gaussian functions in σ_h. The result is expected to be maximum when $\sigma_h = 0$, i.e. when the image is perfectly focused. Since the frequency distribution of the texture is random, the widths of the Gaussian functions are also random. Using the central limit theorem, the result of applying the Laplacian operator to an image point may be assumed to be a Gaussian function of the defocusing parameter σ_h. This general behavior is expected irrespective of the focus measure operator used (see [5], [10]).

In the context of textured images, the Laplacian poses a problem as a focus measure operator. Note that in the case of the Laplacian the second derivatives in the x and y directions can have opposite signs and tend to cancel each other. In the case of textured images, similar instances may occur frequently and the Laplacian may at times behave in a unstable manner. We overcome this problem by defining the *modified Laplacian* as:

$$\nabla^2_M I = \left|\frac{\partial^2 I}{\partial x^2}\right| + \left|\frac{\partial^2 I}{\partial y^2}\right| \quad (12)$$

Note that the modified Laplacian is always greater or equal in magnitude to the Laplacian.

The discrete approximation to the Laplacian is usually a 3×3 operator. In order to accommodate for possible variations in the size of texture elements, we compute the partial derivatives by using a variable spacing (*step*) between the pixels used to compute the derivatives. Hence, the discrete approximation to the modified Laplacian is computed as:

$$\begin{aligned} ML(x,y) = & \quad (13) \\ & |\ 2I(x,y) - I(x-step,y) - I(x+step,y)\ | \\ + & |\ 2I(x,y) - I(x,y-step) - I(x,y+step)\ | \end{aligned}$$

Finally, the focus measure at a point (i,j) is computed as the sum of modified Laplacian values, in a small window around (i,j), that are greater than a threshold value:

$$F(i,j) = \sum_{x=i-N}^{i+N} \sum_{y=j-N}^{j+N} ML(x,y) \quad for\ ML(x,y) \geq T_1 \quad (14)$$

where the parameter N determines the window size used to compute the focus measure. In contrast to auto-focusing methods, we typically use a small window of size 3×3 or 5×5, i.e. $N = 1$ or $N = 2$. We shall refer to the above focus measure as the *sum-modified-Laplacian* (SML). Note that as a result of definition of the modified Laplacian and the use of the threshold T_1, the SML is not a linear operator and cannot be implement as a convolution. However, the SML can be computed using a simple algorithm.

6 Focus Measure Function

The focus measure function at any given image point may be denoted by $F(d)$; SML focus measure as a function of the distance of the corresponding surface point from the focused plane (Fig.3). From section 3, we know that peak of $F(d)$ can be modeled as a Gaussian function[5] with mean value $\overline{d}$ and standard deviation σ_F (Fig.4). This is also experimentally verified in [10]. The mean $\overline{d}$ corresponds to the stage displacement at which $F(d)$ is maximum, i.e.

[5] In general, the fringes of the focus measure function deviate from the Gaussian distribution since the magnification of the imaging system can vary substantially from one fringe to the other [10]. For this reason, we confine ourselves to variations around the peak.

$F(\overline{d}) = F_p$. As the texture content on the surface element increases, F_p increases and σ_F decreases. Each surface element, therefore, is expected to have its own F_p and σ_F values.

The Gaussian model enables us to compute depth from a small number of focus measures by interpolation. We show in the following section that a minimum of *three* focus measures are needed perform the Gaussian interpolation. Since the Gaussian model is valid only in the peak region of $F(d)$, these three focus measures must be computed in this region. In our experiments, we select the displacement parameter Δd such that the above condition is always satisfied.

7 Depth Estimation

We now describe the estimation of depth of a surface point (x, y) from the focus measure set $\{F(d_i) \mid i = 1, 2, ...M\}$ computed at (x, y). The parameter $\overline{d}$ represents the depth of the surface point. For convenience the notation F_i is used to represent the focus measure value $F(d_i)$.

The depth estimation algorithm uses the Gaussian distribution to model the peak region of the focus measure function $F(d)$ and interpolates the computed measure values to obtain accurate depth estimates. The algorithm uses only three focus measures, namely, F_{m-1}, F_m, and F_{m+1}, that lie on the largest mode[6] of $F(d)$, such that, $F_m \geq F_{m-1}$ and $F_m \geq F_{m+1}$ (Fig.4).

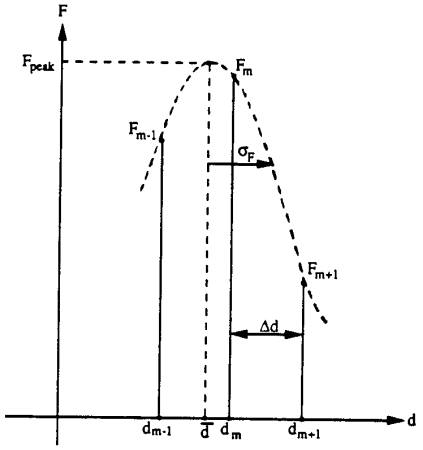

Figure 4: Gaussian interpolation of focus measures.

Using the Gaussian model, the focus measure function may be expressed as:

$$F = F_p \; exp \left\{ -\frac{1}{2}\left(\frac{d - \overline{d}}{\sigma_F}\right)^2 \right\} \qquad (15)$$

where $\overline{d}$ and σ_F are the mean and standard deviation of the Gaussian distribution (Fig.4). Using natural logarithm, we can rewrite eq. 15 as:

$$ln F = ln F_p - \frac{1}{2}\left(\frac{d - \overline{d}}{\sigma_F}\right)^2 \qquad (16)$$

By substituting each of the three measures F_{m-1}, F_m, and F_{m+1}, and its corresponding displacement value in eq. 16, we obtain three equations that can be solved for $\overline{d}$ and σ_F:

$$\overline{d} = \frac{(ln F_m - ln F_{m+1})(d_m{}^2 - d_{m-1}{}^2)}{2\Delta d\{(ln F_m - ln F_{m-1}) + (ln F_m - ln F_{m+1})\}} - \frac{(ln F_m - ln F_{m-1})(d_m{}^2 - d_{m+1}{}^2)}{2\Delta d\{(ln F_m - ln F_{m-1}) + (ln F_m - ln F_{m+1})\}} \qquad (17)$$

$$\sigma_F{}^2 = -\frac{(d_m{}^2 - d_{m-1}{}^2) + (d_m{}^2 - d_{m+1}{}^2)}{2\{(ln F_m - ln F_{m-1}) + (ln F_m - ln F_{m+1})\}} \qquad (18)$$

Using eq.15, we can find F_p from σ_F and $\overline{d}$ as:

$$F_p = F_m \,/\, exp \left\{ -\frac{1}{2}\left(\frac{d_m - \overline{d}}{\sigma_F}\right)^2 \right\} \qquad (19)$$

If F_p is large and σ_F is small, the focus measure function has a strong peak, indicating high surface texture content in the vicinity of the image point (x, y). Hence, the values of F_p and σ_F can be used to segment the observed scene into regions of different texture content.

The following algorithm first finds the measures F_{m-1}, F_m, and F_{m+1} that correspond to the strongest peak of $F(d)$, and then uses these measures to estimate the depth $\overline{d}$ by Gaussian interpolation.

Algorithm

Step 1: Let $k = 3$, $F_{m-1} = 0$, $F_m = 0$, $F_{m+1} = 0$, $d_m = 0$.

Step 2: If $F_{k-1} > F_m$, $F_{k-1} > F_k$, and $F_{k-1} > F_{k-2}$, then:

$F_m = F_{k-1}$
$F_{m-1} = F_{k-2}$
$F_{m+1} = F_k$
$d_m = d_{k-1}$

Step 3: If $k < M$, $k = k + 1$, go to step 2.

Step 4: $d_{m-1} = d_m - \Delta d$ and $d_{m+1} = d_m + \Delta d$. Determine $\overline{d}$, σ_F, and F_p using Eqs. 17, 18, and 19.

Step 5: If $F_p < T_3$ or $\sigma_F > T_4$, the image point (x, y) belongs to background. Stop.

Since the values of F_p and σ_F are only useful for texture segmentation, their evaluation may be avoided to save computations. The algorithm may be applied either in parallel or sequentially to all image points to obtain a dense depth map of the object.

8 An Automated System

We have implemented a fully automated shape from focus system for the recovery of microscopic objects. A photograph of the system is shown in Fig.5. A Nikon Alphaphot-2 model microscope is used to image the objects. Objects

[6] Due to image noise and variations in magnification, the focus measure function may be multi-modal with one strong peak and one or more weak ones.

can be magnified using objective lenses with ×10, ×40, and ×100 magnification. The object is illuminated using bright field illumination where light energy is focused on the object by the same lenses that are used to magnify the object. A CCD camera with 512×512 pixels is mounted on the microscope to obtain digital images of the object. The z-axis of the microscope stage is driven by a stepper motor and the position of the stage can be computer controlled with a resolution and accuracy of 0.02 μm. The shape from focus algorithm is programmed and executed on a Sun SPARC 2 workstation.

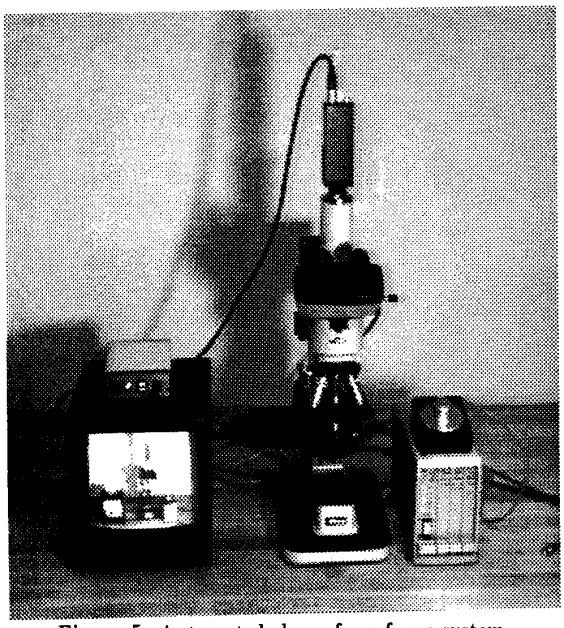

Figure 5: Automated shape from focus system.

The object is placed on the microscope stage and the appropriate objective lens is used to magnify the object. The focus measure parameters (T_1 and *step*) and the stage displacement (Δd) are provided to the program. The program then automatically increments the stage position, digitizes and stores an image for each new position, and uses the image sequence to compute a depth map of the object. The program also reconstructs a focused image of the object from the sequence of defocused images. The reconstruction algorithm uses the estimated depth map to locate and patch together the best focused image areas in image sequence.

The automated system has been used to recover the shapes of a variety of industrial samples. Fig.6 shows a tungsten paste filling in a via-hole on a ceramic substrate [11]. The filling is used to establish electrical connections between different components on a circuit board. The via-hole shown in Fig.6 is approximately 70 μm in diameter and is not sufficiently filled with tungsten paste. A total of 18 images of the via-hole were obtained using stage position increments of $4\mu m$. Some of these images are shown in Fig.6(a-f). The specular reflectance and variable size of the tungsten particles gives the surface a random texture. The white background is the substrate area that has weak texture. Fig.6(g) and Fig.6(h) show the reconstructed image and two views of a depth map obtained using the Gaussian interpolation algorithm.

The above result as well as several other results [10] show that the Gaussian interpolation algorithm performs stably over a wide range of textures. In [10], we have included a quantitative analysis of the errors in computed depth. The automated system is currently being used to compute depth maps and focused images of a variety of industrial as well as medical samples.

Acknowledgements

The author would like to thank Yasuo Nakagawa of PERL, Hitachi, and Reg Willson of the VASC Group, CMU, for several discussions and valuable comments. The author also thanks Ushir Shah for his contribution to the implementation of the automated system.

References

[1] B.K.P. Horn, *Focusing,* MIT Artificial Intelligence Laboratory, Memo No. 160, May, 1968.

[2] J.M. Tenenbaum, *Accommodation in Computer Vision,* Ph.D. Thesis, Stanford University, 1970.

[3] R.A. Jarvis, *Focus optimization criteria for computer image processing,* Microscope, Vol. 24, No. 2, pp. 163-180, 1976.

[4] J.F. Schlag, A.C. Sanderson, C.P. Neumann, F.C. Wimberly, *Implementation of automatic focusing algorithms for a computer vision system with camera control,* Carnegie Mellon University, CMU-RI-TR-83-14, August, 1983.

[5] E. Krotkov, *Focusing,* International Journal of Computer Vision, Vol. 1, pp. 223-237, 1987.

[6] A. Pentland, *A New Sense for Depth of Field,* IEEE Transactions on Pattern Analysis and Machine Intelligence, Vol. 9, No. 4, pp. 523-531, July 1987.

[7] P. Grossmann, *Depth from Focus,* Pattern Recognition Letters, Vol. 5, pp. 63-69, 1987.

[8] T. Darrell and K. Wohn, *Pyramid Based Depth from Focus,* Proc. CVPR, pp. 504-509, 1988.

[9] M. Subbarao, *Efficient Depth Recovery through Inverse Optics,* Machine Vision for Inspection and Measurement, edited by H. Freeman, Academic Press, 1989.

[10] S. K. Nayar, *Shape from Focus System for Rough Surfaces,* Proc. Image Understanding Workshop, San Diego, January, 1992.

[11] T. Ninomiya, M. Nomoto, Y. Nakagawa, *Automatic 2-1/2D Shape Inspection System for Via-Hole Fillings of Green Sheets by Shadow Image Analysis,* Proc. IEEE Intl. Conf. on Robotics and Automation, pp. 515-520, 1989.

[12] R. G. Willson and S. A. Shafer, *Dynamic Lens Compensation for Active Color Imaging and Constant Magnification Focusing,* Carnegie Mellon University, CMU-RI-TR-91, October, 1991.

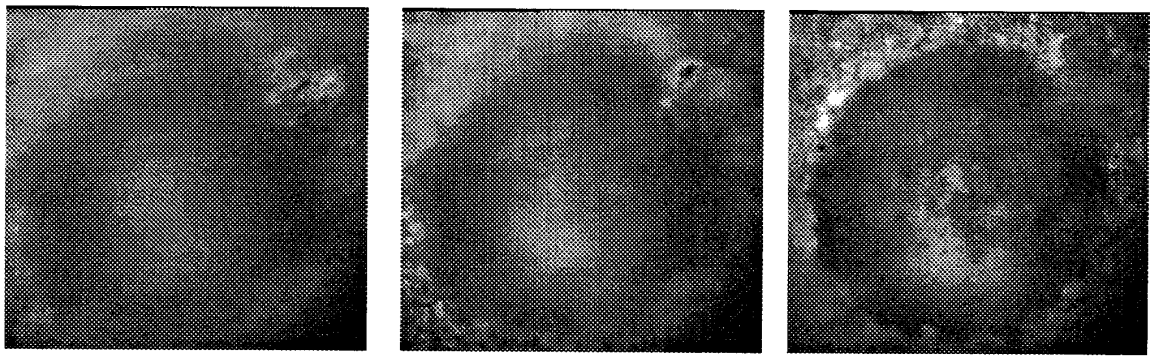

(a) i=2 (b) i=5 (c) i=8

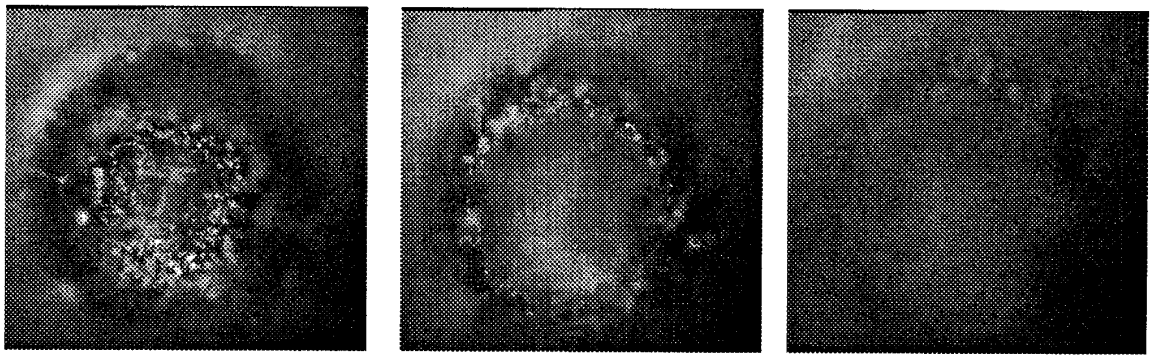

(d) i=11 (e) i=14 (f) i=18

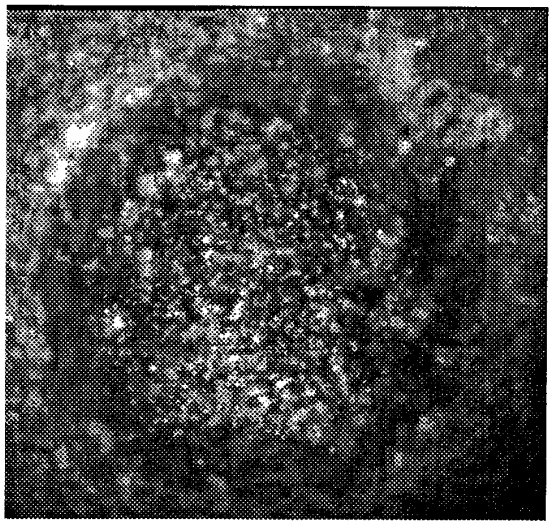

(g) Reconstructed Image

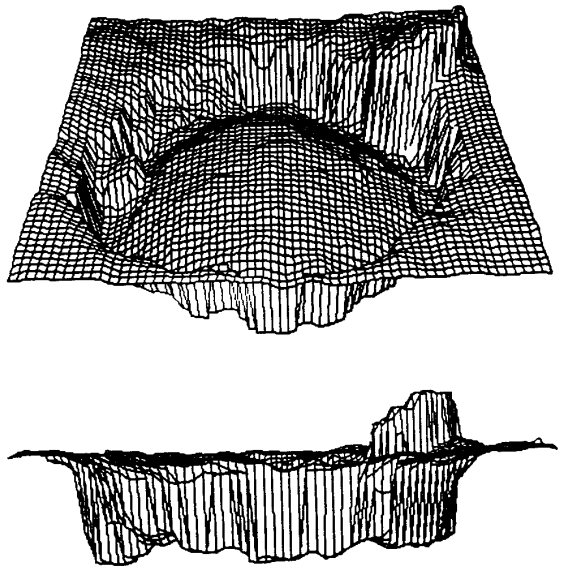

(h) Depth Maps.

Figure 6: Experimental Results: Via-hole filling on ceramic substrate.